High-resolution tropospheric ozone fields for INTEX and ARCTAS from IONS ozonesondes

D. W. Tarasick,[1] J. J. Jin,[2,3] V. E. Fioletov,[1] G. Liu,[1,4] A. M. Thompson,[5] S. J. Oltmans,[6] J. Liu,[1] C. E. Sioris,[1] X. Liu,[7,8] O. R. Cooper,[9,10] T. Dann,[11] and V. Thouret[12]

Received 29 July 2009; revised 11 May 2010; accepted 17 May 2010; published 19 October 2010.

[1] The IONS-04, IONS-06, and ARC-IONS ozone sounding campaigns over North America in 2004, 2006, and 2008 obtained approximately 1400 profiles, in five series of coordinated and closely spaced (typically daily) launches. Although this coverage is unprecedented, it is still somewhat sparse in its geographical spacing. Here we use forward and back trajectory calculations for each sounding to map ozone measurements to a number of other locations and so to fill in the spatial domain. This is possible because the lifetime of ozone in the troposphere is of the order of weeks. The trajectory-mapped ozone values show reasonable agreement, where they overlap, to the actual soundings, and the patterns produced separately by forward and backward trajectory calculations are similar. Comparisons with MOZAIC profiles and surface station data show generally good agreement. A variable-length smoothing algorithm is used to fill data gaps: for each point on the map, the smoothing radius is such that a minimum of 10 data points are included in the average. The total tropospheric ozone column maps calculated by integrating the smoothed fields agree well with similar maps derived from TOMS and OMI/MLS measurements. The resulting three-dimensional picture of the tropospheric ozone field for the INTEX and ARCTAS periods facilitates visualization and comparison of different years and seasons and will be useful to other researchers.

Citation: Tarasick, D. W., et al. (2010), High-resolution tropospheric ozone fields for INTEX and ARCTAS from IONS ozonesondes, *J. Geophys. Res.*, *115*, D20301, doi:10.1029/2009JD012918.

1. Introduction

[2] Ozone plays a major role in the chemical and radiative balance of the troposphere. It controls the oxidizing capacity of the lower atmosphere (it is a primary precursor to the formation of OH radicals) and thereby the capacity of the lower atmosphere to remove other pollutants. Ozone acts as an important infrared absorber (greenhouse gas), particularly in the upper troposphere, and, because of multiple scattering, is more effective in filtering UV-B than its small abundance in the troposphere (about 10% of the total column) would suggest. However, at ground level, ozone is responsible for significant damage to forests and crops and is a principal factor in air quality, as it has adverse effects on human respiratory health [*Jerrett et al.*, 2009].

[3] Ozone soundings are the major source of information on ozone amounts in the free troposphere. When properly prepared and handled, electrochemical concentration cell (ECC) ozonesondes have a precision of 3%–5% and an absolute accuracy of about 10% in the troposphere [*Smit et al.*, 2007; *Kerr et al.*, 1994; *Deshler et al.*, 2008; *Liu et al.*, 2009]. The ozone sensor response time (e^{-1}) of about 25 s gives the sonde a vertical resolution of about 100 m for a typical balloon ascent rate of 4 m/s in the troposphere. Two types of ECC ozonesondes are in current use, the 2Z model manufactured by EnSci Corp. and the 6A model manufactured by Science Pump, with minor differences in construction and some variation in recommended concentrations of the potassium iodide sensing solution and of its phosphate buffer. The maximum variation in tropospheric response

[1]Air Quality Research Division, Environment Canada, Downsview, Ontario, Canada.
[2]Department of Earth and Space Science and Engineering, York University, Toronto, Ontario, Canada.
[3]Now at Jet Propulsion Laboratory, California Institute of Technology, Pasadena, California, USA.
[4]Now at Space Sciences Laboratory, University of California, Berkeley, California, USA.
[5]Department of Meteorology, Pennsylvania State University, University Park, Pennsylvania, USA.
[6]NOAA Climate Monitoring and Diagnostics Laboratory, Boulder, Colorado, USA.
[7]Goddard Earth Sciences and Technology Center, University of Maryland, Baltimore, Maryland, USA.
[8]Harvard-Smithsonian Center for Astrophysics, Cambridge, Massachusetts, USA.
[9]Cooperative Institute for Research in Environmental Sciences, University of Colorado, Boulder, Colorado, USA.
[10]NOAA Earth System Research Laboratory, Boulder, Colorado, USA.
[11]Air Quality Research Division, Environment Canada, Ottawa, Ontario, Canada.
[12]Laboratoire d'Aerologie, Centre National de la Recherche Scientifique, Observatoire Midi-Pyrenees, Toulouse, France.

Table 1. IONS-04 Sites for the July 1 to 15 August 2004 Study Period

Sounding Site	Location			No. of Profiles	Release Time	
	Lat (°N)	Long (°W)	Alt (m)		UT	LST
Canada						
Egbert, ON	44.23	79.78	251	5	11	6
Sable Is., NS	43.93	60.01	4	33	23	18
Yarmouth, NS	43.87	66.12	9	15	17	12
USA						
Ron Brown research vessel, Gulf of Maine	~43.3	~69.5	0	33	15	10
Beltsville, MD	39.04	76.52	24	8	14	9
Boulder, CO	40.30	105.20	1743	7	17	10
Houston, TX	29.87	95.33	19	25	19	13
Huntsville, AL	34.73	86.58	196	14	19	13
Narragansett, RI	41.52	71.32	21	39	18	13
Pellston, MI	45.57	84.68	235	38	18	13
Trinidad Head, CA	41.05	124.15	20	20	18	10
Wallops Is., VA	37.85	75.50	13	18	17	12

resulting from these differences is likely on the order of 2%–3% [*Smit et al.*, 2007].

[4] Although the vertical resolution of ozone soundings is excellent, their geographical and temporal coverage is sparse. Worldwide, there are currently about 60 ozonesonde stations making regular soundings and reporting the data to the World Ozone and Ultraviolet Radiation Data Center (WOUDC; http://www.woudc.org/). Most make weekly soundings. However, during the ICARTT (International Consortium for Atmospheric Research on Transport and Transformation) INTEX (Intercontinental Chemical Transport Experiment) field campaigns (1 July to 15 August 2004), Environment Canada (EC), the National Aeronautics and Space Administration (NASA), the National Oceanic and Atmospheric Administration (NOAA), and several U. S. universities pooled resources to release 275 ozonesondes from a dozen sites across the eastern United States and Canada under the IONS-04 (INTEX Ozonesonde Network Study 2004) program [*Thompson et al.*, 2007a, 2007b]. This represented the largest single set of free tropospheric ozone measurements ever compiled (as of 2004) for this region.

[5] A second IONS campaign, IONS-06, was carried out in 2006, to complement the INTEX-B and TEXAQS aircraft and model studies. This campaign provided more complete coverage of North America, with more sites and launches: a total of 740 sonde profiles were taken from 23 sites.

[6] In 2008, the ARC-IONS (ARCTAS Intensive Ozonesonde Network Study) campaign was undertaken in cooperation with the NASA project Arctic Research of the Composition of the Troposphere from Aircraft and Satellites (ARCTAS), with sites in Canada, Alaska, Greenland, and the northern United States. It consisted of two phases (April and July) with 17 sites, most launching daily, for a total of more than 380 profiles.

[7] The IONS coordinated intensive observational campaigns have provided a unique set of ozone profile measurements over North America. The data have been used extensively to study tropospheric ozone processes and their contribution to the ozone budget [e.g., *Cooper et al.*, 2006, 2007; *Thompson et al.*, 2007a, 2007b, 2008; *Tarasick et al.*, 2007; *Pfister et al.*, 2008; *Yorks et al.*, 2009] for validation of satellite measurements [*Parrington et al.*, 2008, 2009; *Stajner et al.*, 2008; *Schoeberl et al.*, 2007; *Nassar et al.*, 2008; *Jiang et al.*, 2007; *Dupuy et al.*, 2009; *Livingston et al.*, 2007; *Nardi et al.*, 2008] and for initialization and validation of models [*Chai et al.*, 2007; *Pierce et al.*, 2007, 2009; *Yu et al.*, 2007; *Tang et al.*, 2008].

[8] Although the geographical and temporal coverage of the IONS measurements is more than 5 times greater than that of regular network launches, it is still somewhat sparse in its geographical spacing. However, as the lifetime of ozone in the troposphere is of the order of weeks, a measurement of ozone mixing ratio at one place and time also provides an good estimate of ozone mixing ratio in that same air parcel several hours or days before and after. It is therefore possible to employ a technique that has been used successfully in the stratosphere [*Sutton et al.*, 1994; *Newman and Schoeberl*, 1995; *Morris et al.*, 2000] and use forward and back trajectory calculations for each sounding to map ozone measurements to a number of other locations and so to fill in the spatial domain. In the troposphere, trajectories have larger errors than in the stratosphere [*Stohl and Seibert*, 1997], primarily because of the importance of vertical motion, which is difficult to compute accurately, but also because of turbulence in the boundary layer. Nevertheless, trajectory-based domain-filling models have been used successfully to extend ozone climatologies based on MOZAIC aircraft data [*Stohl et al.*, 2001], to reconstruct tropospheric water vapor fields [*Pierrehumbert*, 1998; *Pierrehumbert and Roca*, 1998; *Dessler and Minschwaner*, 2007], and to analyze small-scale variations in ozone mixing ratio observed by research aircraft [*Methven et al.*, 2003].

2. Data and Method

2.1. Ozonesonde Profiles

[9] During the three IONS campaigns ozonesonde profile, data were collected at the sites described in Tables 1–3. At all sites electrochemical concentration cell (ECC) ozonesondes were used, either the 2Z model manufactured by EnSci Corp. or the 6A model manufactured by Science Pump, with some variation in concentration of the KI sensing solution and of its phosphate buffer. Sounding frequency varied, from as often as twice daily to as little as weekly, as may be seen from the column indicating the number of available profiles for each site. Sonde release times also varied between sites but were generally constant, within a campaign, for each site. In general sonde releases were timed to coincide with satellite overpasses and with the maximum in the diurnal cycle of tropospheric ozone (~1–3 p.m. local standard time), except where prescribed by operational weather service requirements (as for many of the Canadian sites, which launch at 11 or 23 UT).

2.2. Data Mapping

[10] Ozone profile data were first converted to 1 km altitude resolution. Ozone partial pressures were averaged for 1 km layers starting at sea level, where altitude was calculated from the measured temperature profile using the hydrostatic relation. These were then divided by the average

Table 2. IONS-06 Sites for the March to May (INTEX-B) and August 2006 Study Periods

Sounding Site	Location			No. of Profiles			Release Time	
	Lat (°N)	Long (°W)	Alt (m)	March	April–May	August	UT	LST
			Canada					
Bratt's Lake, SK	50.20	104.70	580	2	30	29	21	15
Edmonton, AB	53.55	114.11	766	3	4	4	11	4
Egbert, ON	44.23	79.78	251	3	5	15	19	14
Kelowna, BC	49.93	119.40	456	2	26	27	23	15
Sable Is., NS	43.93	60.01	4			28	23	18
Walsingham, ON	42.64	80.60	200		21	20	1,13	20,8
Yarmouth, NS	43.87	66.12	9	3	5	13	23	18
			USA					
Ron Brown research vessel, Gulf of Mexico	~29.0	~95.0	0			38	18	12
Barbados	13.20	59.50	0			27	17	13
Beltsville, MD	39.04	76.52	24			12	18	13
Boulder, CO	40.30	105.20	1743	4	5	34	19	12
Holtville, CA	32.80	115.40	−19			20	20	12
Houston, TX	29.72	95.40	19	17	7	19	20	14
Huntsville, AL	35.28	86.58	196	11	3	33	18	12
Narragansett, RI	41.52	71.32	21	2	13	30	17	12
Paradox, NY	43.92	73.64	284			5	19	14
Socorro, NM	34.6	106.9	1402			27	19	12
Table Mountain, CA	34.40	117.70	2285	3	2	31	20	12
Trinidad Head, CA	41.05	124.15	20	6	15	31	20	12
Valparaiso, IN	41.50	87.00	240		15	5	19	14
Wallops Is., VA	37.87	75.50	13	5	7	11	17	12
Richland, WA	46.20	119.16	123		24		21	13
			Mexico					
Mexico City	19.42	98.58	2272	14		21	18	12

pressure in the layer to produce values for average ozone mixing ratio. The tropopause height was calculated for each profile according to the *World Meteorological Organization* [1992] criterion, that is, the lowest height at which the temperature lapse rate falls to 2°C/km or less, provided that the average lapse rate for 2 km above this height is also not more than 2°C/km. The layer containing the tropopause and those above were not used.

[11] For each location, at 1 km height intervals (0.5 km, 1.5 km, etc.) forward and back trajectories were calculated using version 4.8 of the HYSPLIT model [*Draxler and Hess*, 1997, 1998], developed by the NOAA Air Resources Laboratory (NOAA ARL). The meteorological input for the trajectory model was the global NOAA-NCEP/NCAR (National Centers for Environmental Prediction/National Center for Atmospheric Research) pressure level reanalysis data set. Each trajectory was calculated for 96 h duration, and the original data were mapped to the locations calculated for every 6 h along the forward and back trajectories. In this way, each original measurement was mapped into 32 additional ozone mixing ratio values.

[12] As a quality check, maps produced using only forward trajectories or only back trajectories were compared. These showed, in a few cases, anomalous differences that could be traced to measurements near particularly strong ozone sources. At such points, rapid local ozone production can overwhelm the contribution from advection. The local measurement is therefore not representative of past history, and the back trajectory mapping of the measured ozone is invalid. Such back trajectories were removed. (The forward trajectory-mapped values were presumed still valid.) Although all five IONS campaigns and all levels were similarly examined, only a small number of back trajectories needed to be removed, primarily from the Houston area, Mexico City, and Holtville, CA, in the summers of 2004 and 2006.

[13] The original and trajectory-mapped data were then averaged into bins measuring 1° latitude by 1° longitude, at each 1 km altitude, for the duration of each campaign (~1 month in each case). Two different altitude coordinates were employed for this binning, and so two sets of maps

Table 3. ARC-IONS Sites for the April and July 2008 Study Periods

Sounding Site	Location			No. of Profiles		Release Time	
	Lat (°N)	Long (°W)	Alt (m)	April	July	UT	LST
			Canada				
Bratt's Lake, SK	50.20	104.70	580	15	14	21	15
Churchill, MB	58.74	94.07	30	17	10	23	17
Edmonton, AB	53.55	114.11	766	19	16	23	16
Egbert, ON	44.23	79.78	251		11	18	13
Eureka, NU	79.99	85.94	10	19	1	23	18
Goose Bay, NL	53.32	60.30	44		15	23	19
Kelowna, BC	49.93	119.40	456	13	14	23	15
Resolute, NU	74.71	94.97	46	17	2	23	17
Sable Is., NS	43.93	60.01	4	12	15	23	18
Whitehorse, YT	60.70	135.07	704	12	15	23	15
Yarmouth, NS	43.87	66.12	9		15	23	18
Yellowknife, NT	62.50	114.48	210		19	19	12
			USA				
Barrow, AK	71.32	156.60	11	20		21	12
Boulder, CO	40.30	105.20	1743		13	19	12
Narragansett, RI	41.52	71.32	21	4	3	16	11
Summit, Greenland	72.57	38.48	3238	19	18	14	11
Trinidad Head, CA	41.05	124.15	20	18	17	19	11

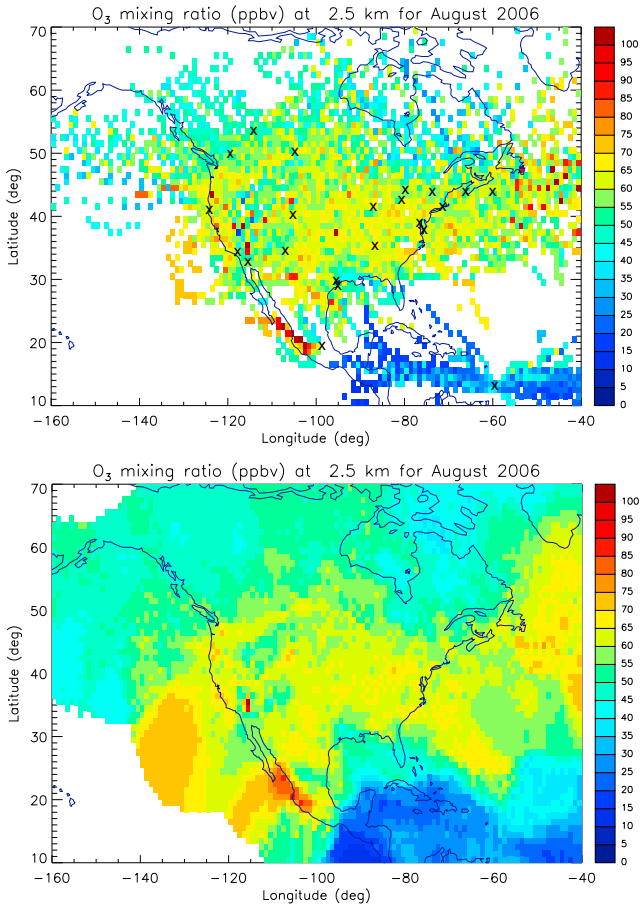

Figure 1. (top) Trajectory-mapped ozone field at 2–3 km above ground level, from the IONS soundings for August 2006. The original data set is 480 soundings from 22 sites. The individual (1° × 1°) pixel averages are shown. The locations of the sounding sites contributing data to this map are also indicated. (bottom) Smoothed version of the ozone field in the upper figure (see text).

were produced: one binned by altitude above sea level and the other binned by altitude above ground level.

[14] Both sets of maps are presented with and without smoothing. For the smoothed maps, a variable-length smoothing algorithm is employed: each 1 × 1° pixel on the map is replaced by the simple average of all data points within a radius of 1°–10°, the smoothing radius being made just large enough that a minimum of 10 data points are included in each average. The parameters of 10° radius (1–2 correlation lengths for ozone in the troposphere) and 10 points are evidently somewhat arbitrary and were determined empirically. Where the data density is high, these parameters imply that for some pixels no smoothing is applied. No average is calculated for locations that do not have 10 data points within a 10° radius.

2.3. Accuracy

[15] The accuracy of these results depends upon the accuracy of the calculated trajectories and also on the assumption that ozone chemistry can be neglected over a 4-day time scale. The latter assumption is generally valid, since the average lifetime of ozone is about 22 days in the troposphere [*Stevenson et al.*, 2006], although it varies with latitude, altitude, and season [*von Kuhlmann et al.*, 2003; *Roelofs and Lelieveld*, 1997]. However, as is well known, in pollution plumes photochemistry can produce ozone on time scales of a few days [e.g., *Mao et al.*, 2006], so this assumption can be violated in certain circumstances, as described below.

[16] A number of studies have attempted to estimate the accuracy of trajectories by several different methods. *Downey et al.* [1990] estimate typical errors of 350 km for 4 day trajectories based on estimated wind errors. *Stohl* [1998] gives a comprehensive review of studies using balloons, material tracers, smoke plumes, and Saharan dust to evaluate trajectory errors and quotes typical errors of 20% of the trajectory distance or about 100–200 km/d (with wide variation between studies). More recently, *Harris et al.* [2005] evaluate trajectory model sensitivity to uncertainties in input meteorological fields and find uncertainties of 30%–40% of the horizontal trajectory distance or 600–1000 km after 4 days, while *Engström and Magnusson* [2009], using an ensemble analysis method, find typical errors in the northern hemisphere of 350–400 km after 3 days and ~600 km after 4 days.

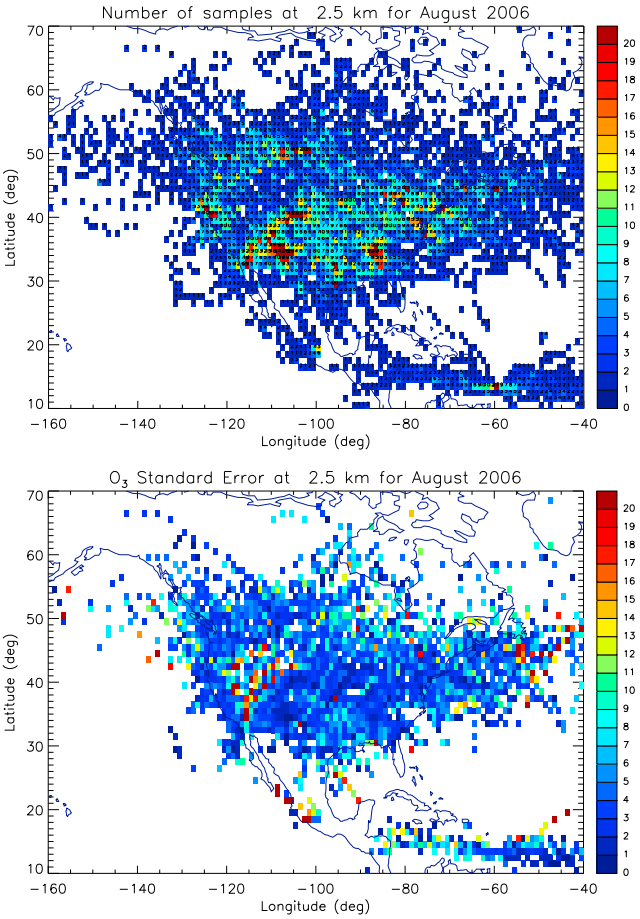

Figure 2. (top) The number of data points contributing to the averages in Figure 1. (bottom) The standard error in ppb for each (1° × 1°) pixel average.

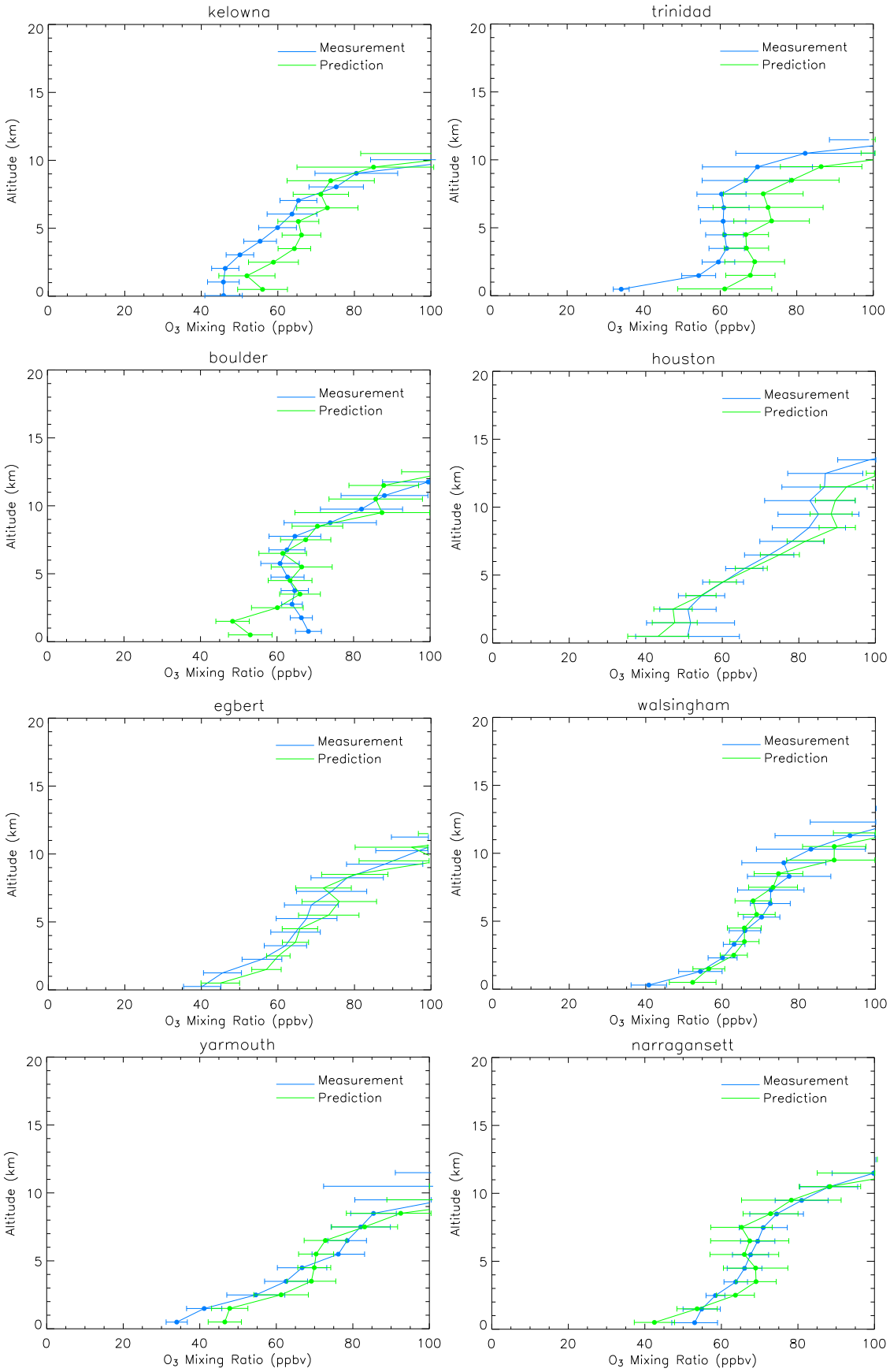
kelowna
trinidad
boulder
houston
egbert
walsingham
yarmouth
narragansett
Measurement
Prediction
Altitude (km)
O3 Mixing Ratio (ppbv)
0
5
10
15
20
0
20
40
60
80
100

Figure 3

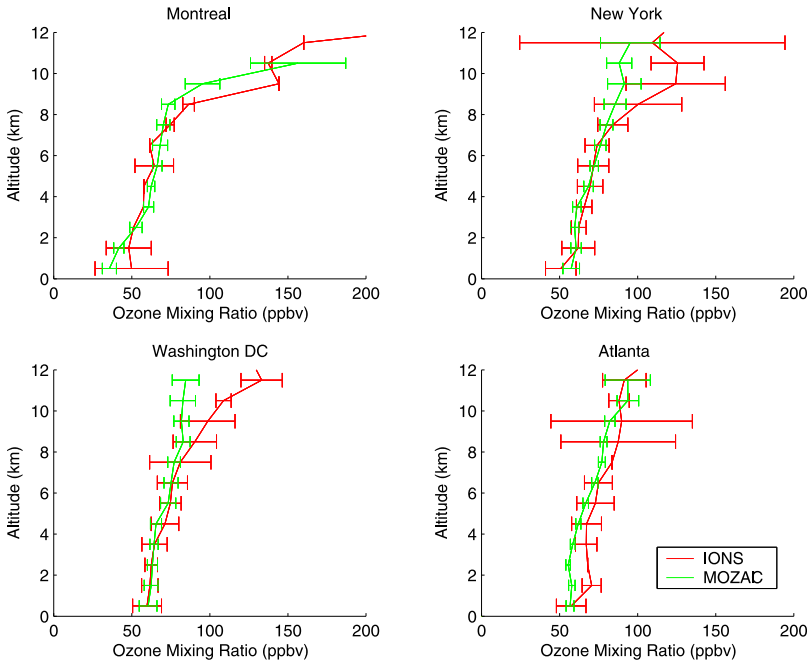

Figure 4. Comparisons between MOZAIC (Measurement of OZone and Water Vapor by AIrbus in-service airCraft) profiles and trajectory-mapped ozone at four North American sites for the July to August 2004 IONS campaign. The error bar half-length is 2 times the standard error of the mean (equivalent to 95% confidence limits on the averages when n is large).

[17] Calculated correlations between ozone values over North America from Aura OMI (Ozone Monitoring Instrument) retrievals [*Liu et al.*, 2005, 2009a, 2009b], and trajectory-mapped ozone soundings at different altitudes (not shown) decrease with time for 1, 2, 3, and 4 days' lag, indicating a decline in accuracy with time (or trajectory length) of the trajectory-mapped ozone values that is consistent with the discussion above; that is, trajectory error increases with time. Correlations are also in general non-negligible even at 4 days' lag. Since this lag is considerably longer, both in time and average trajectory length, than typical correlation time scales (or distances) for ozone in the troposphere [*Liu et al.*, 2009], it implies (as expected based on the discussion above) that the trajectory-mapped values have useful information even after 4 days.

[18] The estimates of ~100–200 km/d quoted above represent errors for individual trajectories in the troposphere. Errors in the final product should be much reduced by averaging of multiple trajectories. However, in the planetary boundary layer (PBL), complex dispersion and turbulence tends to render single trajectories less representative of the actual flow [*Stohl and Seibert*, 1997], and several authors suggest using an ensemble of trajectories [*Merrill et al.*, 1985; *Stohl*, 1998]. In the PBL therefore the averaging of ozone values from multiple trajectories in each pixel, as well as subsequent horizontal averaging (smoothing), will be particularly important for reducing trajectory errors. Nevertheless, we expect results for the lowest (0–1 km) layer to be less accurate than for higher levels.

3. Results and Discussion

3.1. Validation

[19] Figure 1 (top) shows an example of a trajectory-mapped ozone field produced by the procedure described above. The original data set of approximately 480 measurements has been mapped into some 15,800 data values (not precisely 33 × 480, as air parcels do not necessarily remain within an altitude level for the entire 96 h duration of a trajectory). Coverage of North America is quite good, and although there appears to be considerable variation between nearby pixels in some cases, the map shows features expected of the ozone distribution at this altitude: high values near Mexico City and over the Atlantic Ocean off the eastern seaboard, and low values over northern Canada and very low values over the Caribbean. Higher values over the Rocky Mountains reflect the fact that this map is for 2–3 km above ground level, which is the middle troposphere above the Rockies.

Figure 3. Comparisons between the measured ozonesonde profiles and trajectory-mapped fields for selected IONS-06 sites for the month of August 2006. "Measurement" is the ensemble of measured profiles for that site; "Prediction" is the profile generated from the mapping procedure when data from that site is omitted. The error bars indicate 95% confidence limits on the monthly averages.

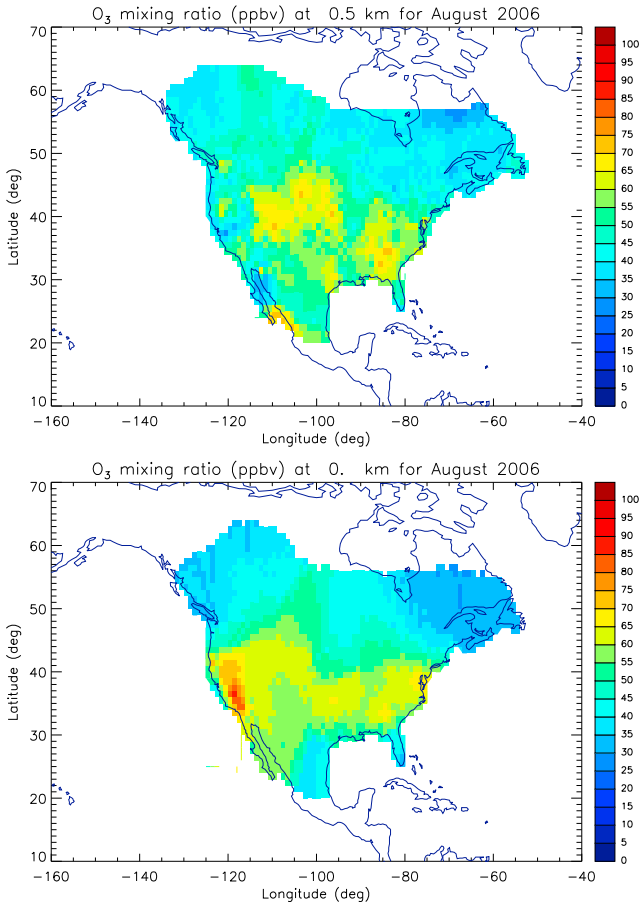

Figure 5. Comparison between the trajectory-mapped ozone field in (top) the lowest kilometer of the atmosphere and (bottom) average mean daily 1 h maximum surface ozone from the NAPS and EPA data bases (1160 sites total) for the month of August 2006. The surface values have been averaged in 1° × 1° bins and smoothed in the same way as the ozonesonde data. Except for central California (where there are no ozonesonde measurements) and northern Mexico (where there are no surface data), the two distributions show fair agreement.

[20] Similar maps, but produced using only forward trajectories or only back trajectories, and therefore comprising half the number of data points (not shown), while not identical, showed similar patterns, permitting some confidence that the averaged results of the trajectory calculations are in general reasonably accurate.

[21] Nevertheless this map appears somewhat "noisy"; that is, it shows small-scale variability that appears random, particularly in areas where data density is low (Figure 2). Since 1° is much less than typical correlation lengths for ozone in the troposphere [*Liu et al.*, 2009], this implies that some degree of horizontal averaging would improve estimates in such areas. However, such averaging will also flatten or reduce any real features that have sharp gradients. Figure 2 indicates that while many pixels contain only one or a few data points, others have as many as 20. In the former case, the number of data points is too small to produce an accurate estimate of the monthly average, and horizontal smoothing would improve that estimate by including information from adjacent pixels. In the latter case, the estimation error is likely already low, and information from adjacent pixels is not likely to improve the estimate. The smoothing function described in section 2.2 attempts to preserve sharp gradients in the maps where the data density is sufficient to resolve them, while smoothing "noise" (both measurement and/or mapping errors and atmospheric variability) where data density is low. The bottom shows the result of this smoothing applied to the trajectory-mapped ozone field. In addition to filling in data gaps with values that are averages of nearby pixels, the smoothing has indeed reduced some of the small-scale variability where data density is low (off the coast of eastern Canada and in the western United States, for example). In such areas and particularly near the edges of the original data field where there are larger data gaps, the smoothing has generated broad features. In the southern and eastern United States, as well as in the northwestern United States and southwestern Canada, where Figure 2 shows a higher density of data, the smoothed field shows more detail.

[22] As noted earlier, the trajectory-mapped data set from which Figure 1 was generated contains nearly 16,000 values; many of these fall within the same 1° × 1° pixel and so are averaged. Figure 2 shows the number of data values and the standard error of the mean for each pixel average in Figure 1. The standard errors are generally of the order of a few ppbv (bottom), although where data density is low (top) they can be higher.

[23] Probably the most revealing test of an interpolation model is to examine how it performs in areas where no data is available. Figure 3 shows comparisons between the measured ozonesonde profile averages for several IONS-06 sites and the profiles produced by trajectory mapping (not smoothed) when data from that site is omitted. Agreement is generally quite good, with most sites at most levels showing differences that are much smaller than the confidence limits on the averages. Some sites show larger differences at the surface and in the PBL, which is not unexpected since, as noted earlier, trajectories are probably less accurate in the PBL, and photochemical production and loss of ozone is more rapid there. However, at Trinidad Head, on the Pacific coast, and to a lesser extent Kelowna (also a west coast site, but somewhat inland) the interpolation shows a significant negative bias when the measured data from the site itself are removed. At these sites, when the measured data are removed, the interpolation must rely on trajectories from continental sites that have generally higher ozone concentrations, while airflow from the west (the dominant influence in the extratropics) would not be represented, as there were no ozonesonde sites to the west (that is, in the Pacific Ocean). This is much less of an issue when data from these sites are present, since local measurements will dominate the averages. However, at coastal sites distant from measurement sites, this will likely introduce biases since trajectories representing airflow from over the ocean will not be included (as there are no measurement sites over the ocean).

[24] This is illustrated in Figure 4, which shows comparisons for the July to August 2004 IONS campaign between MOZAIC (Measurement of OZone and Water Vapor by AIrbus in-service airCraft) profiles and trajectory-mapped

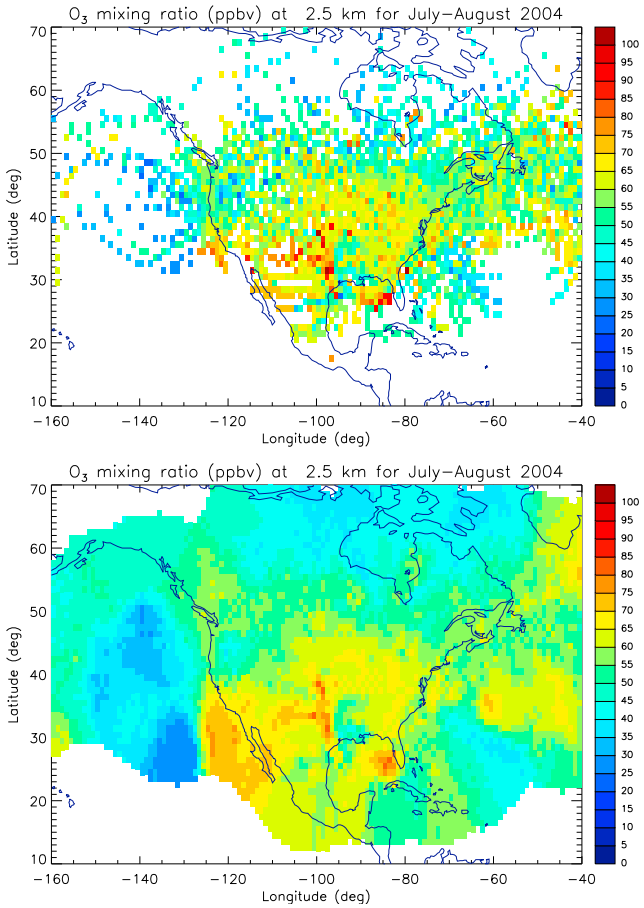

Figure 6. IONS-04 average ozone field for July–August 2004 from trajectory-mapped ozone soundings at 2–3 km altitude: (top) the individual (1° × 1°) pixel averages; (bottom) the smoothed field.

ozone (not smoothed) at four sites in eastern North America. Differences below 10 km are generally within 95% confidence limits on the averages, except for Atlanta. Atlanta is on the coast, and the nearest sounding sites (Houston and Huntsville) are quite distant and inland.

[25] Figure 5 shows a comparison between the (smoothed) trajectory-mapped ozone field for 0–1 km and mean daily 1 h maximum surface ozone from the National Air Pollution Surveillance (NAPS) network Canada-wide data base and the U.S. EPA Air Quality System (AQS) data base (1160 sites total) during the month of August 2006. Mean daily 1 h maximum ozone was chosen as the parameter most similar to the ozone soundings, as the latter were mostly taken in midafternoon. The surface values have been averaged in 1° × 1° bins and smoothed in the same way as the ozonesonde data. The 0–1 km layer is only approximately representative of the PBL, and as remarked above, trajectory errors in the PBL are expected to be larger than in the free troposphere. The surface data are also highly concentrated in California and the eastern United States and sparse through the midwestern United States and Canada; errors in the surface field will be primarily due to linear interpolation in regions of sparse data. Despite these caveats, except for central California (where there are no ozonesonde measurements) and northern Mexico (where there are no surface data), the distribution patterns show evident similarities. A more quantitative comparison, selecting pixels that contain both several surface sites and several trajectory-mapped ozone values (not smoothed), shows a correlation coefficient of about 0.6 for the August 2006 period, if the central California values are excluded. Similar comparisons for the other IONS periods show correlation coefficients generally between 0.6 and 0.7, with the exception of spring 2006, for which the correlation is poor (0.2).

3.2. Examples

[26] Figures 6–9 show examples of trajectory-mapped fields at different altitudes for the other IONS campaigns. Coverage of North America is fairly good. During IONS-04 (which focused on eastern North America), it is less dense in the west, while during IONS-08 (which focused on the Arctic), it is better in the north, but lacking south of about 30°N.

[27] Figures 6 and 7, also for 2–3 km altitude, can be compared with Figure 1. In all three maps, one can clearly see such features as the continental outflow from the southeastern United States (with higher ozone values in April 2006, at this altitude, than in August). Outflow from

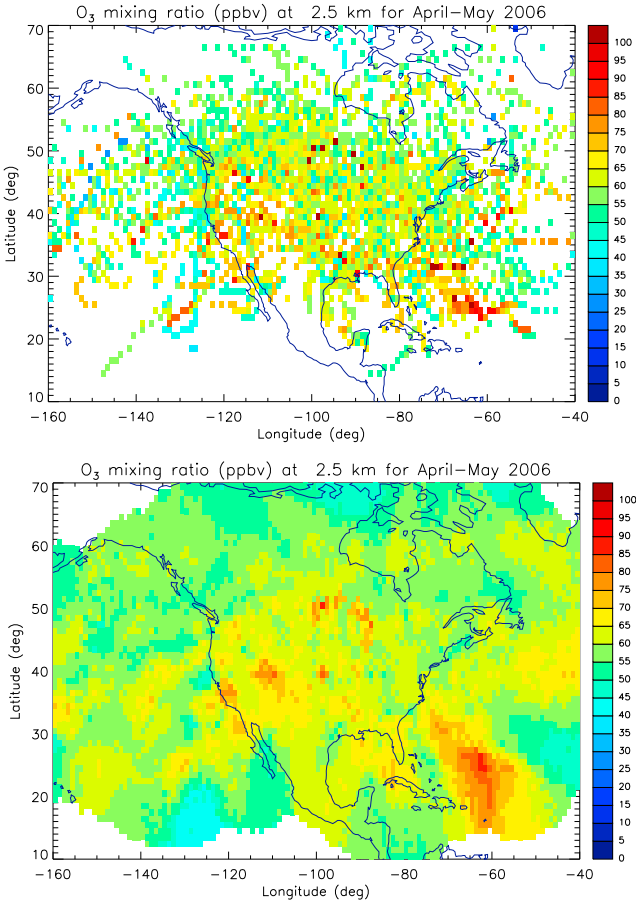

Figure 7. IONS-06 average ozone field for April–May 2006 from trajectory-mapped ozone soundings at 2–3 km altitude: (top) the individual (1° × 1°) pixel averages; (bottom) the smoothed field.

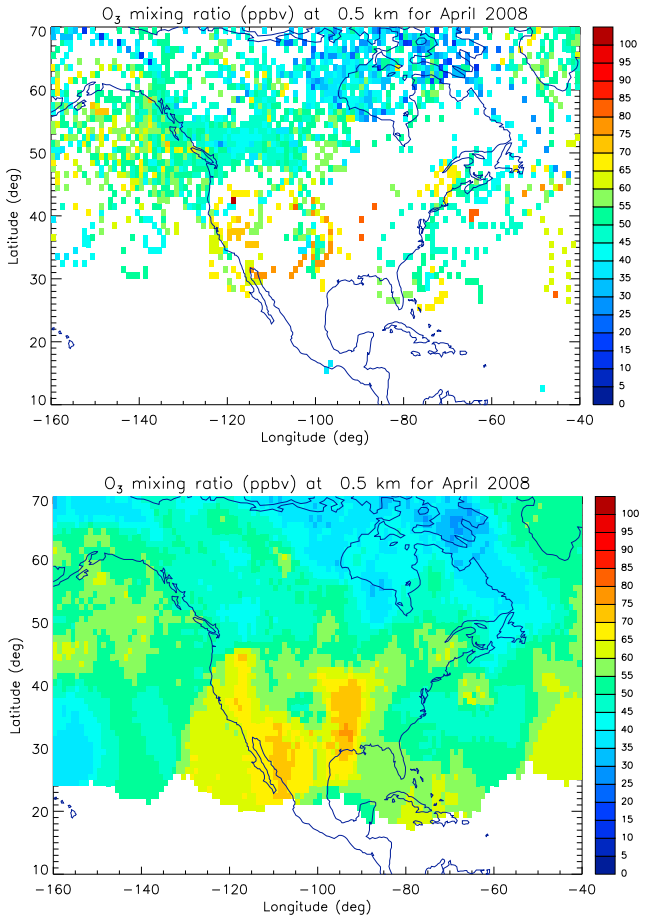

Figure 8. ARC-IONS average ozone field for April 2008 from trajectory-mapped ozone soundings at 0–1 km altitude: (top) the individual (1° × 1°) pixel averages; (bottom) the smoothed field.

the northeastern United States and Canada is also evident in all three maps, but this has higher values in August 2006, and possibly in both summers. However, there is limited sampling off the east coast of Canada in the spring 2006 map (Figure 7), resulting in a smoother field that may be exaggerating the value of these sparse data.

[28] The outflow off the California coast in August 2006 (Figure 1) is present but weaker in 2004 and apparently stronger (more data points further from land) but with lower ozone on average in April to May 2006. In both of the summer figures a number of pixels with ozone values of 70–75 ppb off the coast of California have been interpolated in the smoothed plot to a large and prominent feature, quite possibly exaggerating its importance. Also, in all three figures, features appear to be "stretched" by the smoothing on the edges of the sampling domain, most evidently toward the south. This is again an artifact of the smoothing, which fills in data gaps with the nearest available information. The high ozone feature off the Mexican coast in August 2006 is not seen in other maps, but this is likely because there were no Mexico City ozone soundings in the other data sets.

[29] The eastern continental outflow is much less evident in Figures 8 and 9, as these show fields at 0–1 km and so primarily boundary layer ozone. Comparison of Figure 8 with 9, or Figure 7 with 1, shows that ozone in the free troposphere is considerably higher over northern Canada and the Arctic in April than it is in summer. This is a feature of the ozone climatology over Canada that is well known from the long-term ozonesonde record at several stations [*Logan*, 1999; *Tarasick and Slater*, 2008; *Tarasick et al.*, 1995] but can be seen from these images to be a consistent pattern on a large geographic scale.

3.3. Comparison With Satellite Tropospheric Ozone Column Fields

[30] Figure 10 shows the tropospheric ozone column (TOC) field for August 2006, obtained by integrating the smoothed IONS-06 fields, like that shown in Figure 1. This can be compared with the August 2006 TOC field over North America derived from OMI/MLS observations [*Ziemke et al.*, 2006; see http://acdb-ext.gsfc.nasa.gov/Data_services/cloud_slice/]. The correspondence between the two is further evidence that the trajectory mapping is distributing ozone in the horizontal correctly: the ozonesonde-derived fields show clearly the continental outflow (high ozone over the Atlantic, and to lesser extent, over the Pacific), as well as the southeast-northwest gradient of ozone. Significant features appear in the same places in both maps

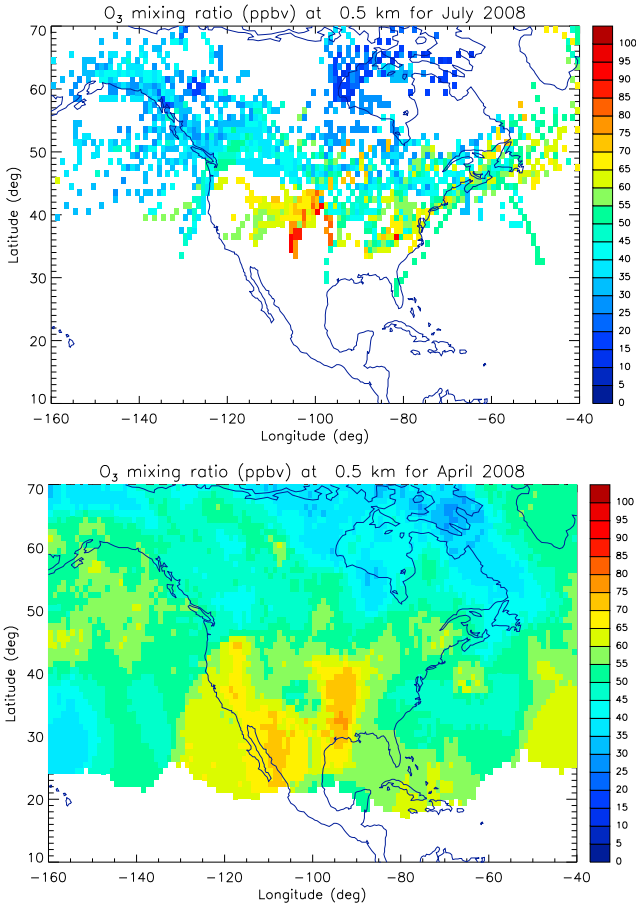

Figure 9. ARC-IONS average ozone field for July 2008 from trajectory-mapped ozone soundings at 0–1 km altitude: (top) the individual (1° × 1°) pixel averages; (bottom) the smoothed field.

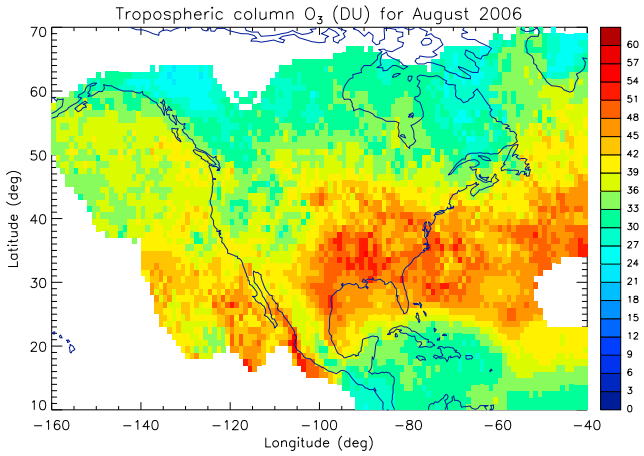

Figure 10. TOC field for August 2006 calculated by integrating the smoothed IONS-06 fields, like that shown in Figure 1 (bottom).

and gradients appear to be of similar magnitude; however, there is a fairly constant bias of 5–10 DU, which is probably due to differences in tropopause height determination.

[31] The TOC fields for the other IONS periods, obtained by integrating the smoothed IONS fields (not shown) also show patterns that compare well with the TOC fields derived from OMI/MLS observations [*Ziemke et al.*, 2006; see http://acdb-ext.gsfc.nasa.gov/Data_services/cloud_slice/], and for the IONS-04 period, with that derived by subtracting the SBUV measurement of stratospheric ozone from the TOMS total ozone column [*Fishman et al.*, 2003; see http://asd-www.larc.nasa.gov/TOR/TOR_Data_and_Images.html]. This comparison is not intended to be quantitative, as the data averaging periods are not exactly the same, and the TOC values depend significantly on the definition of the tropopause and the data averaging method. Nevertheless, the qualitative agreement is a further validation of our trajectory-mapping method, and it is particularly encouraging to see the agreement over the oceans, where no in situ ozone measurements are normally available.

4. Conclusions

[32] A spatial domain-filling technique using forward and back trajectory calculations, applied to the large sets of ozone soundings during the IONS campaigns over North America in 2004, 2006, and 2008, has been shown to produce self-consistent maps of the tropospheric ozone distribution at 1° × 1° horizontal and 1 km vertical resolution. Profiles sampled at some distance from the sounding sites show good agreement with coincident MOZAIC aircraft profiles. The ozone distribution in the lowest kilometer of the atmosphere also shows fair agreement with measurements at surface sites, although there are significant differences due to sampling and local emission sources. The total tropospheric ozone column maps calculated by integrating the smoothed fields agree well with similar maps derived from TOMS and OMI/MLS measurements.

[33] Although results for the lowest 1 km of the atmosphere are likely less accurate, as trajectories are less accurate in the PBL, it appears that overall the most important errors are of representativeness: where significant source regions (like central California or Mexico) are poorly sampled or at coastal sites where only continental trajectories are available. This illustrates the importance in strategic network design of choosing sites that are representative of important airflow regimes.

[34] The resulting three-dimensional picture of the tropospheric ozone field for the INTEX and ARCTAS periods facilitates visualization of regional patterns and the processes they reflect, as well as comparison of different years and seasons. In addition to studies based on the ozone fields themselves, it is expected that these maps will be useful to other researchers, as background information for (aircraft and model) process studies, and for initialization and validation of models. The maps and data files are available for download on the WOUDC Web site, http://www.woudc.org.

[35] **Acknowledgments.** We thank the many observers who obtained the measurements at the sites used in this study. Their careful work is gratefully acknowledged. We thank J. Witte, who archived all of the IONS data in near-real time. We also thank J. Davies, R. Mittermeier, and T. Mathews for assistance with data processing. Data were obtained from the World Ozone and Ultraviolet Radiation Data Center (WOUDC) operated by Environment Canada, Toronto, Ontario, Canada, under the auspices of the World Meteorological Organization. Funding of the IONS ozonesondes was provided by Environment Canada; NOAA; NASA; U. S. EPA; Max Plank Institute for Chemistry, Mainz; Los Alamos National Laboratory; Valparaiso University; the University of Rhode Island; the California Department of Energy; the California Air Resources Board; and the Friends of the Green Horse Society via a grant from ExxonMobil Canada. The authors also acknowledge the strong support of the European Commission, Airbus, and the airlines (Lufthansa, Austrian, Air France) who carry and maintain the MOZAIC equipment free of charge since 1994. MOZAIC is presently funded by INSU-CNRS (France), Meteo-France, and Forschungszentrum Julich (Germany). The MOZAIC data base is supported by ETHER (CNES and INSU-CNRS).

References

Chai, T., et al. (2007), Four-dimensional data assimilation experiments with International Consortium for Atmospheric Research on Transport and Transformation ozone measurements, *J. Geophys. Res.*, *112*, D12S15, doi:10.1029/2006JD007763.

Cooper, O. R., et al. (2006), Large upper tropospheric ozone enhancements above midlatitude North America during summer: In situ evidence from the IONS and MOZAIC ozone monitoring network, *J. Geophys. Res.*, *111*, D24S05, doi:10.1029/2006JD007306.

Cooper, O. R., et al. (2007), Evidence for a recurring upper tropospheric ozone maximum above eastern North America during summer, *J. Geophys. Res.*, *112*, D23304, doi:10.1029/2007JD008710.

Deshler, T., et al. (2008), Atmospheric comparison of electrochemical cell ozonesondes from different manufactures, and with different cathode solution strengths: The balloon experiment on standards for ozonesondes (BESOS), *J. Geophys. Res.*, *113*, D04307, doi:10.1029/2007JD008975.

Dessler, A. E., and K. Minschwaner (2007), An analysis of the regulation of tropical tropospheric water vapor, *J. Geophys. Res.*, *112*, D10120, doi:10.1029/2006JD007683.

Downey, A., J. D. Jasper, J. Gras, and S. Whittlestone (1990), Lower tropospheric transport over the Southern Ocean, *J. Atmos. Chem.*, *11*, 43–68, doi:10.1007/BF00053667.

Draxler, R. R., and G. D. Hess (1997), Description of the HYSPLIT_4 modeling system, *NOAA Technical Memorandum ERL ARL-224*, December, 24 pp.

Draxler, R. R., and G. D. Hess (1998), An overview of the HYSPLIT_4 modeling system for trajectories, dispersion and deposition, *Aust. Met. Mag.*, *47*, 295–308.

Dupuy, E., et al. (2009), Validation of ozone measurements from the Atmospheric Chemistry Experiment (ACE), *Atmos. Chem. Phys.*, *9*, 287–343.

Engström, A., and L. Magnusson (2009), Estimating trajectory uncertainties due to flow dependent errors in the atmospheric analysis, *Atmos. Chem. Phys. Discuss.*, *9*, 15,747–15,767.

Fishman, J., A. E. Wozniak, and J. K. Creilson (2003), Global distribution of tropospheric ozone from satellite measurements using the empirically corrected tropospheric ozone residual technique: Identification of the regional aspects of air pollution, *Atmos. Chem. Phys.*, *3*, 893–907, doi:10.5194/acp-3-893-2003.

Harris, J. M., R. R. Draxler, and S. J. Oltmans (2005), Trajectory model sensitivity to differences in input data and vertical transport method, *J. Geophys. Res.*, *110*, D14109, doi:10.1029/2004JD005750.

Jerrett, M., R. T. Burnett, C. A. Pope III, K. Ito, G. Thurston, D. Krewski, Y. Shi, E. Calle, and M. Thun (2009), Long-term ozone exposure and mortality, *N. Engl. J. Med.*, *360*, 1085–1095.

Jiang, Y., et al. (2007), Validation of aura microwave limb sounder ozone by ozonesonde and lidar measurements, *J. Geophys. Res.*, *112*, D24S34, doi:10.1029/2007JD008776.

Kerr, J. B., et al. (1994), The 1991 WMO international ozonesonde intercomparison at Vanscoy, Canada, *Atmos.-Ocean*, *32*, 685–716.

Liu, G., D. W. Tarasick, V. E. Fioletov, C. E. Sioris, and Y. J. Rochon (2009), Ozone correlation lengths and measurement uncertainties from analysis of historical ozonesonde data in North America and Europe, *J. Geophys. Res.*, *114*, D04112, doi:10.1029/2008JD010576.

Liu, X., K. Chance, C. E. Sioris, R. J. D. Spurr, T. P. Kurosu, R. V. Martin, and M. J. Newchurch (2005), Ozone profile and tropospheric ozone retrievals from the Global Ozone Monitoring Experiment: Algorithm description and validation, *J. Geophys. Res.*, *110*, D20307, doi:10.1029/2005JD006240.

Liu, X., P. K. Bhartia, K. Chance, R. J. D. Spurr, and T. P. Kurosu (2009a), Ozone profile retrievals from the Ozone Monitoring Instrument, *Atmos. Chem. Phys. Discuss.*, *9*, 22,693–22,738.

Liu, X., P. K. Bhartia, K. Chance, T. P. Kurosu, and R. J. D. Spurr (2009b), Validation of OMI ozone profiles and stratospheric ozone columns with microwave limb sounder, *Atmos. Chem. Phys. Discuss.*, *9*, 24,913–24,943.

Livingston, J., et al. (2007), Comparison of water vapor measurements by airborne Sun photometer and near-coincident in situ and satellite sensors during INTEX/ITCT 2004, *J. Geophys. Res.*, *112*, D12S16, doi:10.1029/2006JD007733.

Logan, J. A. (1999), An analysis of ozonesonde data for the troposphere: Recommendations for testing 3-D models and development of a gridded climatology for tropospheric ozone, *J. Geophys. Res.*, *104*(D13), 16,115–16,149, doi:10.1029/1998JD100096.

Mao, H., R. Talbot, D. Troop, R. Johnson, S. Businger, and A. M. Thompson (2006), Smart balloon observations over the North Atlantic: O_3 data analysis and modeling, *J. Geophys. Res.*, *111*, D23S56, doi:10.1029/2005JD006507.

Merrill, J., R. Bleck, and L. Avila (1985), Modeling Atmospheric Transport to the Marshall Islands, *J. Geophys. Res.*, *90*(D7), 12,927–12,936, doi:10.1029/JD090iD07p12927.

Methven, J., S. R. Arnold, F. M. O'Connor, H. Barjat, K. Dewey, J. Kent, and N. Brough (2003), Estimating photochemically produced ozone throughout a domain using flight data and a Lagrangian model, *J. Geophys. Res.*, *108*(D9), 4271, doi:10.1029/2002JD002955.

Morris, G. A., J. F. Gleason, J. Ziemke, and M. R. Schoeberl (2000), Trajectory mapping: A tool for validation of trace gas observations, *J. Geophys. Res.*, *105*(D14), 17,875–17,894, doi:10.1029/1999JD901118.

Nardi, B., et al. (2008), Initial validation of ozone measurements from the High Resolution Dynamics Limb Sounder, *J. Geophys. Res.*, *113*, D16S36, doi:10.1029/2007JD008837.

Nassar, R., et al. (2008), Validation of tropospheric emission spectrometer (TES) Nadir ozone profiles using ozonesonde measurements, *J. Geophys. Res.*, *113*, D15S17, doi:10.1029/2007JD008819.

Newman, P. A., and M. R. Schoeberl (1995), A reinterpretation of the data from the NASA Stratosphere-Troposphere Exchange Project, *Geophys. Res. Lett.*, *22*(18), 2501–2504, doi:10.1029/95GL02220.

Parrington, M., D. B. A. Jones, K. W. Bowman, L. W. Horowitz, A. M. Thompson, D. Tarasick, and J. C. Witte (2008), Constraining the summertime tropospheric ozone distribution over North America through assimilation of observations from the Tropospheric Emission Spectrometer, *J. Geophys. Res.*, *113*, D18307, doi:10.1029/2007JD009341.

Parrington, M., D. B. A. Jones, K. W. Bowman, A. M. Thompson, D. W. Tarasick, J. Merrill, S. J. Oltmans, T. Leblanc, J. C. Witte, and D. B. Millet (2009), Impact of the assimilation of ozone from the Tropospheric Emission Spectrometer on surface ozone across North America, *Geophys. Res. Lett.*, *36*, L04802, doi:10.1029/2008GL036935.

Pfister, G. G., L. K. Emmons, P. G. Hess, J.-F. Lamarque, A. M. Thompson, and J. E. Yorks (2008), Analysis of the Summer 2004 ozone budget over the United States using Intercontinental Transport Experiment Ozonesonde Network Study (IONS) observations and Model of Ozone and Related Tracers (MOZART-4) simulations, *J. Geophys. Res.*, *113*, D23306, doi:10.1029/2008JD010190.

Pierce, R. B., et al. (2007), Chemical data assimilation estimates of continental U. S. ozone and nitrogen budgets during the Intercontinental Chemical Transport Experiment–North America, *J. Geophys. Res.*, *112*, D12S21, doi:10.1029/2006JD007722.

Pierce, R. B., et al. (2009), Impacts of background ozone production on Houston and Dallas, Texas, air quality during the Second Texas Air Quality Study field mission, *J. Geophys. Res.*, *114*, D00F09, doi:10.1029/2008JD011337.

Pierrehumbert, R. (1998), Lateral mixing as a source of subtropical water vapor, *Geophys. Res. Lett.*, *25*(2), 151–154, doi:10.1029/97GL03563.

Pierrehumbert, R., and R. Roca (1998), Evidence for control of Atlantic subtropical humidity by large scale advection, *Geophys. Res. Lett.*, *25*(24), 4537–4540, doi:10.1029/1998GL900203.

Roelofs, G.-J., and J. Lelieveld (1997), Model study of the influence of cross-tropopause O_3 transports on tropospheric O_3 levels, *Tellus Ser. B*, *49*, 38–55.

Schoeberl, M. R., et al. (2007), A trajectory based estimate of the tropospheric column ozone column using the residual method, *J. Geophys. Res.*, *112*, D24S49, doi:10.1029/2007JD008773.

Smit, H. G. J., et al. (2007), Assessment of the performance of ECC-ozonesondes under quasi-flight conditions in the environmental simulation chamber: Insights from the Juelich Ozone Sonde Intercomparison Experiment (JOSIE), *J. Geophys. Res.*, *112*, D19306, doi:10.1029/2006JD007308.

Stajner, I., et al. (2008), Assimilated ozone from EOS-Aura: Evaluation of the tropopause region and tropospheric columns, *J. Geophys. Res.*, *113*, D16S32, doi:10.1029/2007JD008863.

Stevenson, D. S., et al. (2006), Multimodel ensemble simulations of present day and near-future tropospheric ozone, *J. Geophys. Res.*, *111*, D08301, doi:10.1029/2005JD006338.

Stohl, A. (1998), Computation, accuracy and applications of trajectories – A review and bibliography, *Atmos. Environ.*, *32*, 947–966.

Stohl, A., and P. Seibert (1997), Accuracy of trajectories as determined from the conservation of meteorological tracers, *Q. J. R. Meteorol. Soc.*, *124*, 1465–1484, doi:10.1002/qj.49712454907.

Stohl, A., P. James, C. Forster, N. Spichtinger, A. Marenco, V. Thouret, and H. G. J. Smit (2001), An extension of Measurement of Ozone and Water Vapour by Airbus In-service Aircraft (MOZAIC) ozone climatologies using trajectory statistics, *J. Geophys. Res.*, *106*, 27,757–27,768, doi:10.1029/2001JD000749.

Sutton, R. T., H. Maclean, R. Swinbank, A. O'Neill, and F. W. Taylor (1994), High-resolution stratospheric tracer fields estimated from satellite observations using Lagrangian trajectory calculations, *J. Atmos. Sci.*, *51*, 2995–3005.

Tang, Y., et al. (2008), The impact of chemical lateral boundary conditions on CMAQ predictions of tropospheric ozone over the continental United States, *Environ. Fluid Mech.*, *9*, 43–58, doi:10.1007/s10652-008-9092-5.

Tarasick, D. W., and R. Slater (2008), Ozone in the troposphere: Measurements, climatology, budget, and trends, *Atmos.-Ocean*, *46*, 93–115, doi:10.3137/ao.460105.

Tarasick, D. W., D. I. Wardle, J. B. Kerr, J. J. Bellefleur, and J. Davies (1995), Tropospheric ozone trends over Canada: 1980–1993, *Geophys. Res. Lett.*, *22*(4), 409–412, doi:10.1029/94GL02991.

Tarasick, D. W., et al. (2007), Comparison of Canadian air quality forecast models with tropospheric ozone profile measurements above mid-latitude North America during the IONS/ICARTT Campaign: Evidence for stratospheric input, *J. Geophys. Res.*, *112*, D12S22, doi:10.1029/2006JD007782.

Thompson, A. M., et al. (2007a), Intercontinental chemical transport experiment Ozonesonde Network Study (IONS) 2004: 1. Summertime upper troposphere/lower stratosphere ozone over northeastern North America, *J. Geophys. Res.*, *112*, D12S12, doi:10.1029/2006JD007441.

Thompson, A. M., et al. (2007b), Intercontinental chemical transport experiment Ozonesonde Network Study (IONS) 2004: 2. Tropospheric ozone budgets and variability over northeastern North America, *J. Geophys. Res.*, *112*, D12S13, doi:10.1029/2006JD007670.

Thompson, A. M., J. E. Yorks, S. K. Miller, J. C. Witte, G. A. Morris, D. Baumgardner, L. Ladino, and B. Rappenglueck (2008), Tropospheric ozone sources and wave activity over Mexico City and Houston during Milagro/Intercontinental Transport Experiment (INTEX-B) Ozonesonde Network Study, 2006 (IONS-06), *Atmos. Chem. Phys.*, *8*, 5113–5125.

von Kuhlmann, R., M. G. Lawrence, P. J. Crutzen, and P. J. Rasch (2003), A model for studies of tropospheric ozone and nonmethane hydrocarbons: Model description and ozone results, *J. Geophys. Res.*, *108*(D9), 4294, doi:10.1029/2002JD002893.

World Meteorological Organization (1992), International meteorological vocabulary, *WMO Rep. 182*, World Meteorol. Org., Geneva, Switzerland.

Yorks, J. E., A. M. Thompson, E. Joseph, and S. K. Miller (2009), The variability of free tropospheric ozone budgets over Beltsville, Maryland (39N, 77W) in the summers 2004–2007, *Atmos. Environ.*, *43*, 1827–1838.

Yu, S., R. Mathur, K. Schere, D. Kang, J. Pleim, and T. L. Otte (2007), A detailed evaluation of the Eta-CMAQ forecast model performance for O_3, its related precursors, and meteorological parameters during the 2004 ICARTT study, *J. Geophys. Res.*, *112*, D12S14, doi:10.1029/2006JD007715.

Ziemke, J. R., S. Chandra, B. N. Duncan, L. Froidevaux, P. K. Bhartia, P. F. Levelt, and J. W. Waters (2006), Tropospheric ozone determined from Aura OMI and MLS: Evaluation of measurements and comparison with the Global Modeling Initiative's Chemical Transport Model, *J. Geophys. Res.*, *111*, D19303, doi:10.1029/2006JD007089.

O. R. Cooper, Cooperative Institute for Research in Environmental Sciences, University of Colorado, Boulder, CO 80309, USA.

T. Dann, Air Quality Research Division, Environment Canada, 335 River Road, Ottawa, ON, Canada K1V 1C7.

V. E. Fioletov, J. Liu, C. E. Sioris, and D. W. Tarasick, Air Quality Research Division, Environment Canada, Downsview, ON, Canada M3H 5T4. (david.tarasick@ec.gc.ca)

J. J. Jin, Jet Propulsion Laboratory, California Institute of Technology, 4800 Oak Grove Drive, Mail Stop 183-701, Pasadena, CA 91109, USA.

G. Liu, Space Sciences Laboratory, 7 Gauss Way 7450, University of California, Berkeley, CA 94720-7450, USA.

X. Liu, Goddard Earth Sciences and Technology Center, University of Maryland, Baltimore County, 5523 Research Park Drive, Suite 320, Baltimore, MD 21228, USA.

S. J. Oltmans, NOAA Climate Monitoring and Diagnostics Laboratory, 325 Broadway, Boulder, CO 80305, USA.

A. M. Thompson, Department of Meteorology, 510 Walker Building, Pennsylvania State University, University Park, PA 16802, USA.

V. Thouret, Laboratoire d'Aerologie, Centre National de la Recherche Scientifique, Observatoire Midi-Pyrenees, 14 Av. E. Belin, 31400, Toulouse, France.